Interactions between the Cell Cycle and Embryonic Patterning in *Arabidopsis* Uncovered by a Mutation in DNA Polymerase ε [W][OA]

Pablo D. Jenik,[a] Rebecca E.J. Jurkuta,[b] and M. Kathryn Barton[a,1]

[a] Department of Plant Biology, Carnegie Institution, Stanford, California 94305
[b] Department of Genetics, University of Wisconsin, Madison, Wisconsin 53706

Pattern formation and morphogenesis require coordination of cell division rates and orientations with developmental signals that specify cell fate. A viable mutation in the *TILTED1* locus, which encodes the catalytic subunit of DNA polymerase ε of *Arabidopsis thaliana*, causes a lengthening of the cell cycle by ~35% throughout embryo development and alters cell type patterning of the hypophyseal lineage in the root, leading to a displacement of the root pole from its normal position on top of the suspensor. Treatment of preglobular and early globular stages, but not later stage, embryos with the DNA polymerase inhibitor aphidicolin leads to a similar phenotype. The results uncover an interaction between the cell cycle and the processes that determine cell fate during plant embryogenesis.

INTRODUCTION

Cell type specification and cell division are closely coordinated in the development of multicellular organisms. The identity of the cells determines how long their cell cycle is and when and how often they divide and in which orientation. Tissue-specific differences in cell cycle length are common and important for normal development. One example of this is the differential rates of cell division in the central and peripheral zones of the shoot meristem of plants. For instance, see Davis et al. (1979) for work on sunflower (*Helianthus annuus*) and Reddy et al. (2004) for more recent work on the mustard *Arabidopsis thaliana*. It is less clear to what extent the converse is true (i.e., how much cell division influences cell type specification in the plant). Manipulations of the cell cycle by overexpressing cell cycle regulators result in a variety of phenotypes, from having no effect on the morphology of the plant to severely affecting organ growth and shape (reviewed in Jakoby and Schnittger, 2004).
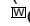
Cell division cycle and patterning are coordinated during plant embryogenesis, when the basic body plan of the organism is established. Most dicotyledonous embryos go through similar developmental stages, globular-shape, heart-shape, and torpedo-shape, and are patterned similarly. Organ and tissue types are distributed along two perpendicular axes. The vasculature, endodermis, cortex, and epidermis are arranged along the radial (inside–outside) axis, while the shoot meristem, hypocotyl, root, and root meristem lie along the shoot–root (apical–basal) axis (Natesh and Rau, 1984). Ho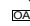wever, there is considerable diversity in embryonic cell division patterns among dicotyledonous embryos. In some species, such as cotton (*Gossypium hirsutum*), cell divisions during embryogenesis follow no predictable pattern (Pollock and Jensen, 1964). In other species, such as *Arabidopsis*, the cell division pattern is extremely regular (Mansfield and Briarty, 1991). Thus, in some species, the sequence and orientation of cell divisions and the cell fate decisions are tightly coregulated, while in others, patterning is superimposed on what appears to be relatively disorganized cell division patterns. By and large, the regular pattern of cell divisions is not absolutely required for *Arabidopsis* embryonic development. Mutants that display drastic changes in the orientation of the cell division plane, such as *tonneau1* (*ton1*), *fass/ton2*, and *auxin-resistant 6*, result in embryos that are, broadly speaking, correctly patterned (proper apical–basal and radial axes established). In spite of this, the mutant seedlings die shortly after germination or produce very abnormal plants (Mayer et al., 1993; Shevell et al., 1994; Torres-Ruiz and Jürgens, 1994; Traas et al., 1995; Hobbie et al., 2000). In addition, manipulating the cell cycle by expressing a dominant negative form of cyclin-dependent kinase A from a late embryogenesis promoter (*At2S2*) (Hemerly et al., 2000) or antisense *cyclinA3;2* from a constitutive promoter (*TetO*) (Yu et al., 2003) results in seedlings with a variety of morphological defects, suggesting that the regulation of the cell cycle and the pattern of cell divisions are both important for the formation of normal embryos and plants.

Central to the cell cycle are molecules responsible for replicating nuclear DNA during the S-phase. In eukaryotic cells, three replicative DNA polymerase (DNA pol) holoenzymes are involved in this process. DNA pol α/primase synthesizes the short primers for the Okazaki fragments on the lagging strand and is a likely target of checkpoint control. DNA pols δ and ε copy the bulk of the chromosomal DNA. DNA pols δ and ε may play distinct roles in DNA replication, since both proteins are essential in yeast (*Saccharomyces cerevisiae*) and *Caenorhabditis elegans* (Encalada et al., 2000; Fraser et al., 2000; Hübscher et al., 2002). Mutations in DNA pols can alter cell cycle duration, with

profound effects in the cell fate and patterning of organisms. For instance, a mutation (*div-1*) or RNA interference (RNAi) of subunits of DNA pol α/primase or RNAi of DNA pol δ in *C. elegans* results in longer cell cycles. The change in cell cycle length affects the fate of the endodermal and mesodermal lineages and results in lethality (Encalada et al., 2000; Gönczy et al., 2000). Similar mutations in *Drosophila melanogaster* are either early lethal (strong alleles) or affect eye development (weak alleles) (Chen et al., 2000). Lethal mutations in DNA pol ε have been described recently in *Arabidopsis* (Ronceret et al., 2005).

In this study, we have characterized the embryonic defects of mutants in the catalytic subunit of DNA pol ε of *Arabidopsis*, encoded by the *TILTED1* (*TIL1*) locus. Mutants homozygous for the strong alleles (*til1-1* to *-3*) are embryo lethal. Mutants homozygous for the weak allele (*til1-4*) are viable and have longer cell cycles, delayed development, and larger cells. The longer cell cycles are also correlated with abnormal patterning of the uppermost cell of the suspensor, the hypophysis. This results in an abnormal placement of the root pole. These alterations can be phenocopied by treatment of wild-type embryos with a DNA pol inhibitor.

RESULTS

A Mutation in the *TIL1* Locus Slows Embryonic Development and Alters the Placement of the Root Pole

With the goal of identifying new pathways involved in embryo patterning, a line homozygous for the shoot apical meristem–expressed P_{STM}:*GUS* reporter (the promoter of the *SHOOT MERISTEMLESS* gene fused to β-glucuronidase) was mutagenized with ethyl methanesulfonate and screened for embryo-defective mutants (Joy, 2001). One line segregated slowly developing embryos in which the root pole was displaced laterally. This displacement causes the root–shoot axis to be at an angle to the long axis of the suspensor, giving the embryo a tilted appearance (cf. Figures 1I and 1L). The gene was named *TIL1*, and the allele found in this screen was called *til1-4* (see below for naming of alleles).

The development of the *Arabidopsis* embryo is characterized by a very regular series of cell divisions and by the almost synchronous development of all the embryos in the silique (see Supplemental Table 1 online). Self-pollination of a *til1-4* heterozygote plant (*TIL1/til1-4*) produced ~25% slowly developing embryos (138/542). When presumed *til1-4* heterozygotes (plants segregating tilted, delayed embryos) were crossed to the wild type, half of the F1 progeny segregated wild-type embryos, and half segregated tilted, delayed embryos. These results indicate that *til1-4* segregates as a single nuclear recessive mutation.

Delayed mutant embryos remain white as wild-type embryos in the same silique turn green. By late embryogenesis, however, all embryos in the presumed *TIL1/til1-4* plants were green, indicating that the delayed embryos had recovered. Furthermore, no dead or nongerminating seeds were observed in the progeny of presumed *TIL1/til1-4* plants, indicating that homozygous *til1-4* embryos are viable.

When the seeds of a self-pollinated *til1-4* heterozygote were planted to soil, one-quarter of the progeny (16/60) grew more slowly than the wild type. These presumed *til1-4/til1-4* plants had slow growing roots, slightly delayed flowering, altered floral phyllotaxis, a reduced number of ovules, abnormally developing ovules, and reduced fertility. When crossed to the wild type, these presumed *til1-4/til1-4* plants produced only phenotypically wild-type F1 progeny (Table 5). All F1 progeny produced tilted, delayed embryos, indicating that the parents were indeed homozygous for the *til1-4* mutation. These genotypes were later confirmed with an appropriate derived cleaved-amplified polymorphic sequence marker (see Supplemental Table 2 online).

The *til1-4* Mutation Causes Abnormal Division Patterns in the Developing Root of the Embryo

To better understand the cause of the displacement of the root pole, we next examined the development of *til1-4/til1-4* embryos. In wild-type embryos, the zygote divides into an apical cell, which gives rise to the embryo proper, and a basal cell, which produces the extraembryonic suspensor and a portion of the root (Jürgens and Mayer, 1994) (we staged the embryos according to this reference, but using the term "transition" instead of "triangular" stage). By the early globular stage (when the embryo proper is 32 cells), the topmost cell of the suspensor is morphologically distinct and is called the hypophysis (Figure 1A). Soon thereafter, the hypophysis divides transversely to give rise to a smaller lens cell and a basal cell (Figures 1C and 1F). Cells derived from the lens cell (lens cell descendents [lcd]) become the quiescent center (QC) of the root. Cells derived from the basal cell (basal cell descendents [bcd]) undergo additional transverse divisions to form two tiers by the heart stage (Figure 1I) and three tiers by the end of embryogenesis. Together, these tiers make up the central root cap (or columella) and its initials (stem cells). The hypophysis and its progeny together are symmetrically arranged above the suspensor in an upside-down cone shape. After the early globular stage (32 cells), the provascular cells elongate in the direction of the shoot–root axis (Figure 1A). The provascular cells terminate basally at the lcd (Figure 1I).

Mutant embryos, identified by their delayed phenotype, segregating in heterozygous *til1-4* siliques were scored for morphological abnormalities. While *til1-4/til1-4* embryos showed occasional abnormal cell divisions between the 4- and 16-cell stages, consistent defects were seen starting at the early globular stage (see Supplemental Table 1 online). Defects at the root pole involving the hypophysis and its derivatives were grouped into three classes (Table 1). In most *til1-4/til1-4* embryos, the hypophysis divided abnormally during the globular stage. In many cases, it divided longitudinally (class 1: split hypophysis class) (Figure 1B). In other cases, it divided slightly obliquely or nearly normal, but the resulting lens cell was asymmetric or otherwise abnormal in shape (Figures 1D and 1G) (class 2: abnormal lens cell class). The longitudinal division of the lens cell and basal cell occurred too early, during the globular stage instead of the transition stage (Figure 1E). These first two classes may both be interpreted as abnormalities in the plane of the first division of the hypophysis. These first abnormally formed cells divided improperly as development progressed, resulting in
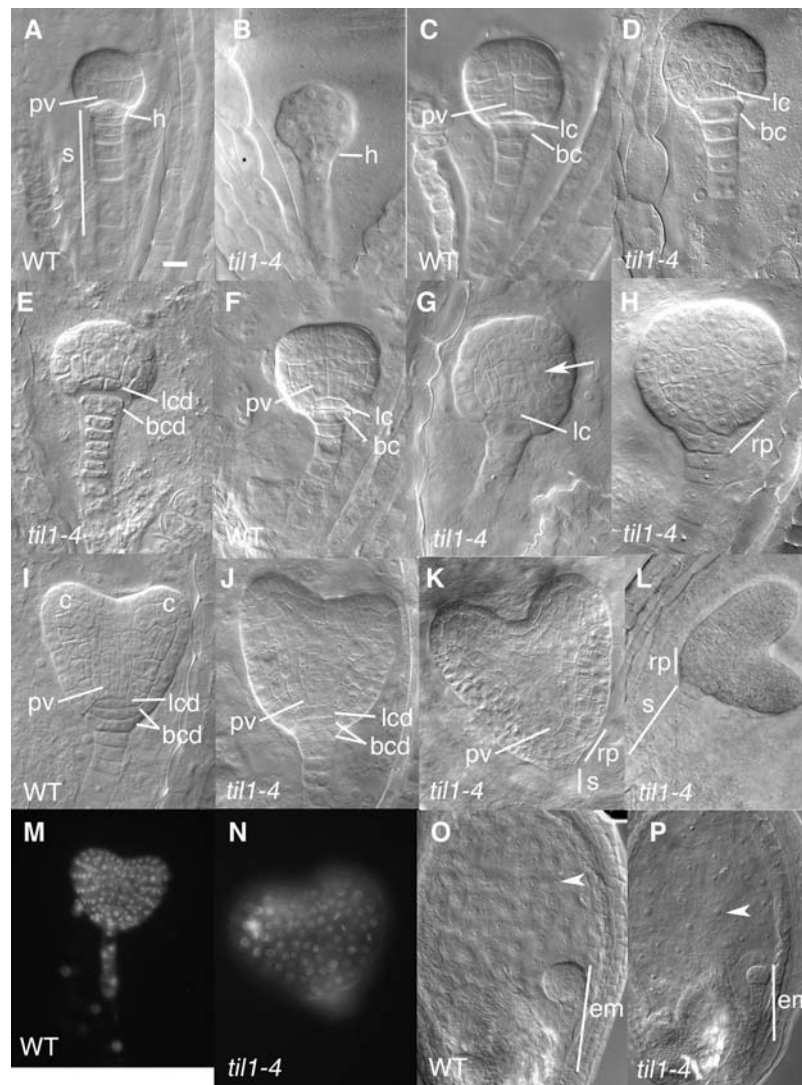
Figure 1. Phenotypes of Wild-Type and Homozygous *til1-4* Embryos.

Note that in all cases, wild-type embryos are compared with *til1-4/til1-4* embryos of similar embryonic stage. The *til1-4/til1-4* embryos develop more slowly and are therefore always chronologically older than their wild-type counterparts. h, hypophysis; s, suspensor; lc, lens cell; lcd, lens cell descendant; bc, basal cell; bcd, basal cell descendants; pv, provascular cells; c, cotyledon; rp, root pole; em, embryo. Bars = 10 μm in **(A)** to **(K)**, 15 μm in **(L)** to **(N)**, and 20 μm in **(O)** and **(P)**.

(A) Wild-type early globular embryo.

(B) *til1-4/til1-4* early globular embryo.

(C) Wild-type mid globular embryo.

(D) and **(E)** *til1-4/til1-4* mid globular embryos. In **(D)**, the lens cell is asymmetric. In **(E)**, both the lens cell and basal cell have divided longitudinally.

(F) Wild-type late globular embryo.

(G) and **(H)** *til1-4/til1-4* late globular embryos. In **(G)**, the lens cell is asymmetric. Cells in the right side of the embryo (arrow) show abnormal divisions.

(I) Wild-type early heart stage embryo. The hypophyseal cell lineage is symmetric.

(J) to **(L)** *til1-4/til1-4* early heart stage embryos. In all three cases, the hypophyseal cell lineage is abnormal. The resulting tilt of the shoot–root axis relative to the suspensor axis varies from slight **(J)** to moderate **(K)** to extreme **(L)**.

(M) and **(N)** Wild-type **(M)** and *til1-4/til1-4* **(N)** DAPI-stained early heart stage embryos.

(O) and **(P)** Wild-type **(O)** and *til1-4/til1-4* **(P)** free nuclear endosperm at 96 h after pollination.

Table 1. Frequencies of Phenotypic Classes of Root Pole Development of Wild-Type and *til1-4/til1-4* Embryos

Phenotypic Class	Early Globular Stage Embryos		Mid Globular Stage Embryos		Late Globular Stage Embryos		Early Heart Stage Embryos	
	Wild Type ($n = 131$)	*til1-4/til1-4* ($n = 67$)	Wild Type ($n = 96$)	*til1-4/til1-4* ($n = 46$)	Wild Type ($n = 93$)	*til1-4/til1-4* ($n = 64$)	Wild Type ($n = 92$)	*til1-4/til1-4* ($n = 57$)
Wild type–looking	100%	20.9%	100%	15.2%	100%	6.2%	96.7%	1.6%
Class 1: split hypophysis	0%	26.9%	0%	41.3%	0%	40.7%	NA[a]	NA
Class 2: abnormal lens cell[b]	0%	52.2%	0%	26.1%	0%	6.2%	1.1%	43.8%
Class 3: abnormal root pole[c]	0%	0.0%	0%	17.4%	0%	46.9%	2.2%	54.6%

Both wild-type and *til1-4/til1-4* embryos were from self-pollinated *TIL1/til1-4* plants.
[a] NA, not applicable. The hypophysis in the wild type has split by this stage.
[b] In these embryos, the lens cell was abnormal, while the bcd were normal or only mildly abnormal.
[c] In these embryos, both the lens cell and the bcd were abnormal.

a root pole that had cells of the wrong shape and in inappropriate positions and sometimes too many cells (Figures 1H and 1K) (class 3: abnormal root pole class). By the heart stage, approximately half of the embryos had only a mildly abnormal root pole, with abnormally shaped lcd and bcd (Table 1, Figure 1J). In the rest of the embryos, when the cotyledons grew out, it was clear that the lcd were displaced from their normal position on top of the suspensor. This was accompanied by the asymmetric development of the provasculature, which is in contact with the lcd at its basal end. This resulted in a shoot–root axis that was at an angle (tilted) with respect to the suspensor (Table 1, Figures 1K and 1L). After the torpedo stage, with the degeneration of the suspensor used as a reference point, the tilting of the axis was no longer evident, although the lcd and bcd were still in abnormal positions. In a fraction of mutant embryos, some cells outside the root pole did not divide properly, usually taking longer to divide than would have been expected for the stage. These defects were more noticeable at the globular stages (25.3% of early globular embryos) (Figure 1G) and much more subtle at the heart stage or later (9% of early heart stage embryos). We occasionally saw extra divisions of the cells of the suspensor, ranging from a few extra cells next to the embryo to a small mass of cells (data not shown). Overproliferation of the suspensor is a common phenotype in embryo-defective mutants (Schwartz et al., 1994).

In summary, the main morphological defect observed in most *til1-4* homozygous embryos was the abnormal division of the hypophysis, generating a lens cell that was abnormal in shape or abnormally positioned, and the asymmetric development of the provasculature. This ultimately led to an abnormal root pole and misplaced lcd and bcd. Abnormal cell divisions in other regions occurred only in a fraction of the mutant embryos and did not have lasting observable consequences.

til1-4/til1-4 Embryos Have Larger Cells and Nuclei Than Wild-Type Embryos but the Same DNA Content

In addition to being delayed, *til1-4/til1-4* embryos were larger than their wild-type counterparts at the same developmental stage (e.g., Figures 1I versus 1J and 1K). While staging the mutant embryos, we observed that their cell number was similar to that of wild-type embryos. The difference in embryo size was thus probably due to an increase in cell size. To confirm this, we measured embryos at the early heart stage, both in length (from the lcd to the notch between the cotyledons) and width (just above the provasculature) and counted the cells along these lines of measurement. We also measured the length of the most basal provascular cell and the width of one of the lcd. The results shown on Table 2 indicate that mutant and wild-type embryos at

Table 2. Embryo and Embryonic Cell Sizes in the Wild Type and *til1-4/til1-4*

Embryo Genotype and Stage (n)	Embryo Length[a]		Embryo Width[a]		Width of QC[a]	Length of First Vascular[a]
	μm	No. of Cells	μm	No. of Cells	μm	μm
Wild type, early heart (25)	44.5 ± 0.6	6.8 ± 0.1	55.0 ± 1.1	10.2 ± 0.1	7.2 ± 0.2	12.2 ± 0.5
til1-4/til1-4, early heart (20)	53.0 ± 1.0[b]	5.9 ± 0.1[c]	71.4 ± 1.6[b]	9.8 ± 0.2	10.2 ± 0.3[b]	15.3 ± 0.7[b]
Wild type, late heart (19) same silique sibs[d]	69.3 ± 1.7	9.3 ± 0.2	75.3 ± 1.0	12.9 ± 0.3	8.0 ± 0.2	12.5 ± 0.5
Wild type, early heart aphidicolin-treated (8)	49.4 ± 1.8[c]	6.5 ± 0.2	63.9 ± 3.2[c]	10.4 ± 0.5	7.8 ± 0.4	14.5 ± 0.5[b]

[a] All values are given ±1 SE of the mean.
[b] Significantly different from wild-type early heart stage embryos ($P < 0.01$, Student's *t* test).
[c] Significantly different from wild-type early heart stage embryos ($P < 0.05$, Student's *t* test).
[d] "Same silique sibs" refers to wild-type embryos of the same age (in the same silique) as the *til1-4/til1-4* early heart embryos.

the same developmental stage contained essentially the same number of cells (the one-cell difference in length is due to a delayed division in some embryos of one of the precursors of the shoot apical meristem), but the cells of the mutant embryos were larger. These cells were also larger than the cells of wild-type embryos of the same age. These data indicated that cells in *til1-4/til1-4* embryos took longer to divide and therefore kept growing longer than the cells in the wild-type embryo before the division occurred. In spite of this delay, patterning was for the most part normal with the exception of the lcd and bcd. The larger cells cause the *til1-4/til1-4* embryos to be significantly larger (*t* test, P < 0.01) than wild-type embryos at the same developmental stage, in both dimensions, but not as large as the wild-type embryos of the same chronological age (i.e., in the same silique).

In many plant cell types, there is a correlation between DNA content and cell size, although this is not always the case (reviewed in Sugimoto-Shirasu and Roberts, 2003). We measured the average size of nuclei in early heart stage embryos and their DNA content. For this, we dissected embryos and stained them with 4′,6-diamidino-2-phenylindole (DAPI). The areas of the nuclei were measured on images taken under a compound microscope (Figures 1M and 1N), and the nuclear volume was calculated assuming spherical dimensions. The nuclei of mutant embryos were significantly larger than the nuclei of wild-type embryos (*t* test, P < 0.01) (Table 3) and stain more diffusely. However, their DNA content (calculated by measuring the intensity of the fluorescence of DAPI stain) was similar (Table 3). While the mutant cells and their nuclei are larger than their wild-type counterparts, there is no concomitant increase in DNA content.

At the end of embryogenesis, *til1-4/til1-4* mutant seeds could be distinguished from wild-type seeds by their size: *til1-4/til1-4* embryos were larger than wild-type embryos (*t* test, P < 0.01) (Table 4). The desiccation of all the seeds in *TIL1/til1-4* siliques occurred at the same time. Since the cells in mutant embryos divided at a slower rate, *til1-4/til1-4* embryos should undergo desiccation with fewer cells than wild-type embryos. To estimate the number of cells in different regions of the embryo at the end of embryogenesis, we counted cells in the cortex of the hypocotyl of 7-d-old light-grown seedlings (these cells do not divide after germination; Gendreau et al., 1997) and in the cortex of the root meristem of 2-d-old seedlings (when very few postgermination cell divisions have occurred; Barrôco et al., 2005). In both cases, there were fewer cells in the mutant (*t* test, P < 0.01) (Table 4). Upon measuring the size of hypocotyl cells in mature embryos

Table 3. Nuclear Size in Wild-Type and *til1-4/til1-4* Embryonic Cells

Embryo Genotype and Stage	Volume (μm³)[a]	DNA Content (Arbitrary Units)[a]
Wild type, early heart	33 ± 0.1 (*n* = 40)	1280 ± 54 (*n* = 40)
til1-4/til1-4, early heart	49 ± 0.3 (*n* = 40)[b]	1138 ± 43 (*n* = 40)

[a] All values are given ±1 SE of the mean. Four embryos were analyzed per genotype.
[b] Significantly different from wild-type embryos (P < 0.01, Student's *t* test).

dissected out of imbibed seeds (Table 4), we concluded that *til1-4/til1-4* embryos, by the end of their development, are larger and have fewer and larger cells than their wild-type counterparts.

In the Early *til1-4/til1-4* Embryos, Asymmetric *SCARECROW* Expression Precedes Asymmetric Auxin Accumulation and the Displacement of the Root Pole

To assess how the morphological abnormalities were correlated with alterations in cell fate and tissue patterning, we crossed *til1-4* to lines containing different tissue-specific markers and tested whether their expression was affected in homozygous mutant embryos. First, we looked at the expression of P_{STM}:*GUS*, which is expressed in the cells that will become the shoot apical meristem, between the cotyledons (Joy, 2001). As stated above, and reflecting the morphology, the expression of this apical marker was normal in *til1-4/til1-4* embryos (Figures 2A and 2B).

We then looked at markers for the root pole, the region most affected in *til1-4/til1-4* embryos. First, we analyzed the gene trap *PIN4:GUS* (*PIN4* is a putative auxin efflux facilitator), which is expressed in the wild-type embryo in the lens cell and in provascular cells apical to it (Figure 2C) and later in the QC cells and cells apical to them (Figure 2E). Expression is always symmetric and centered with respect to the suspensor (Friml et al., 2002). In mutant globular stage embryos, *PIN4:GUS* was still expressed in the same set of cells, but because of their abnormal shape or plane of cell division, some of them were off center (Figure 2D). This displacement of the QC and neighboring cells to one side and the asymmetry of *PIN4:GUS* expression pattern was more apparent in later stage embryos (Figure 2F) and suggested that the whole root pole was off center.

DR5rev is a synthetic promoter that responds to auxin and, with much lower sensitivity, to brassinosteroids (Nakamura et al., 2003). *DR5rev* expression has been suggested as a reporter of high local auxin activity (auxin maxima) (Friml et al., 2003). In wild-type embryos, from the early globular stage onwards, *DR5rev:GFP* was expressed in the hypophysis and its derivatives: the lens cell (Figure 2G) and the lcd that will become QC cells (Figures 2I and 2K) and the basal cell (Figure 2G) and all the tiers of cells derived from it (Figures 2I and 2K). Late in development (and postembryonically), its expression is stronger at the base of the columella (Figure 2K). As with *PIN4:GUS*, *DR5rev:GFP* expression was always symmetric and centered with respect to the suspensor. In *til1-4/til1-4* globular stage embryos, *DR5rev:GFP* was expressed symmetrically with respect to the suspensor in the lcd and bcd, even when these cells had divided abnormally (Figure 2H). However, as the embryos developed, *DR5rev:GFP* expression progressively shifted to one side (Figure 2J) and became markedly asymmetric in many torpedo stage embryos (Figure 2L). The *DR5rev:GFP* expression pattern suggests that the auxin maximum is initially set up in its normal location in *til1-4* mutant embryos but is subsequently shifted laterally.

In many *til1-4/til1-4* embryos, the number of lcd cells expressing the *DR5rev:GFP* marker was reduced (Figures 2J and 2L), suggesting that only some of them had acquired a QC fate. To explore this possibility, we analyzed the marker *QC25*, which is an indicator of QC fate in the embryo and in the root (Sabatini

Table 4. Size and Cell Numbers in Wild-Type and *til1-4/til1-4* Mature Embryos or Seedlings

Embryo or Seedling Genotype	*n* (Embryos)	Embryo Length (μm)[a]	Embryo Width (μm)[a]	*n* (Cells)[b]	Length Epidermal Hypocotyl Cell (μm)[a]	*n* (Seedlings)	Number of Cells (7-d Hypocotyl)[a]	*n* (Seedlings)	Number of Cells (2-d Root Meristem)[a]
Wild type	23	498 ± 8	111 ± 4	60	15.0 ± 0.3	28	26.8 ± 0.4	24	26.0 ± 0.4
til1-4	26	544 ± 8[c]	131 ± 3[c]	60	15.8 ± 0.3[d]	34	24.0 ± 0.4[c]	20	17.5 ± 0.5[c]

[a] All values are given ±1 SE of the mean.
[b] Six embryos were analyzed per genotype.
[c] Significantly different from wild-type embryos/seedlings (P < 0.01, Student's *t* test).
[d] Significantly different from wild-type embryos/seedlings (P < 0.05, Student's *t* test).

et al., 1999). Accordingly, *QC25* in wild-type embryos was expressed in the lens cell (Figure 2M) and later in the four QC cells (Figure 2O). In general, *til1-4/til1-4* embryos had reduced levels of expression of *QC25*. In mutant embryos, *QC25* was also expressed in the lens cell, even if it had an abnormal shape (Figure 2N). Later in development, while approximately half of the embryos (24 out of 41) had the normal complement of QC cells (albeit shifted to one side) (Figure 2P), the other half (17 out of 41) had a reduced number of QC cells (Figure 2Q), confirming our observations with *DR5rev:GFP*. All these results suggest that in *til1-4/til1-4* embryos, the result of the atypical divisions of the hypophysis is the shifting of the whole root pole (QC and associated initials, as indicated by the markers) to an asymmetric position to one side with respect to the suspensor.

Finally, we examined the expression of *P_{SCR}:GFP* (the promoter of the transcription factor *SCARECROW* fused to green fluorescent protein) (Wysocka-Diller et al., 2000). *SCR* has been proposed to be one of the factors that determines the position and identity of the QC (Aida et al., 2004). This marker showed asymmetric expression in the mutant embryos from the inception of its expression. In wild-type embryos, *P_{SCR}:GFP* expression starts in the hypophysis (Figure 2R). After the transverse division of this cell, it is expressed in both the lens cell and the basal cell (Figure 2T). Later, expression disappears from the bcd and is maintained in the lcd, the cortex-endodermis initials, and the endodermal lineage (Figures 2W and 2Y). In most globular *til1-4/til1-4* embryos with a split hypophysis, *P_{SCR}:GFP* was expressed in only one of the two cells (12/15 embryos) (Figure 2S), contrasting with *DR5rev:GFP*, which was expressed in both cells (Figure 2H). Later in development, *P_{SCR}:GFP* was expressed in only one lcd in 9/12 embryos (Figure 2U) and in two lcd in 3/12 embryos (Figure 2V). These two patterns most likely correspond to the embryos with a reduced or normal number of QC cells observed with the other markers. After the early heart stage, *P_{SCR}:GFP* was expressed in an apparently abnormal group of cells at the root pole (Figures 2X and 2Z). Some of these were QC cells, others were the cortex-endodermis initials, but this marker did not allow us to distinguish the two types. *P_{SCR}:GFP* was expressed normally in the endodermal lineages of mutant embryos (Figures 2X and 2Z).

Our results point to a correlation between the asymmetric expression of *SCR* and the displacement of the QC identity. This suggests that the off-center lcd that express SCR are the ones

that acquire QC fate. The displaced QC may subsequently relocalize the auxin maximum, resulting in the observed shift of *DR5rev:GFP* expression and the root pole itself.

TIL1 Encodes the Catalytic Subunit of DNA Pol ε

A map-based cloning approach was used to isolate the locus affected in the *til1-4* mutant. The mutation was mapped to a 44-kb stretch of DNA between the markers *T23G18f* and *T27G7e*, near the top of chromosome I (Figure 3A). This region contained nine annotated genes (*At1g08250* to *At1g08325*). One of these genes, *At1g08260*, was represented in the collection of embryo lethal mutations generated by David Meinke's laboratory, with three T-DNA insertional alleles of this gene, called *emb2284-1* to *-3* (McElver et al., 2001; Tzafrir et al., 2003). Mutants homozygous for any of the three *emb2284* alleles had the same phenotype, with embryos arresting at the early to mid globular stage, sometimes with abnormal divisions in the hypophysis, and then aborting (Figure 4A). We confirmed the allelism among these three mutations by crossing them to each other (data not shown). We then performed complementation tests with *til1-4* and concluded that *til1-4* and *emb2284* are allelic. Approximately one-quarter of the embryos resulting from a cross between *TIL1/til1-4* and *EMB2284/emb2284-1* were delayed and had *til1*-like phenotypes (Table 5, Figure 4B). We obtained the same results when crossing *TIL1/til1-4* plants to *EMB2284/emb2284-2* or *EMB2284/emb2284-3* plants (Figure 4C). In the F1 generation from the complementation cross, one-quarter of the plants had the reduced fertility (and reduced ovule number) phenotype typical of *til1-4/til1-4* plants. All F1 plants showing reduced fertility were *til1-4/emb2284-1 trans*-heterozygotes (Table 6). In addition, the roots of *til1-4/emb2284-1* seedlings grew as slowly as those of *til1-4/til1-4* seedlings (data not shown). These results, besides proving allelism, showed that the *til1-4* allele was dominant over the *emb2284* alleles. In agreement with D. Meinke (personal communication), we decided to rename the *emb2284-1* to *-3* alleles as *til1-1* to *-3* (Figure 3B). We sequenced *At1g08260* from *til1-4/til1-4* plants and found that it contained two G-to-A mutations: one at position 3927 (counting from the first ATG) in exon 12 and one at position 5005 in intron 14. The former mutation changes a conserved Gly (position 472) into an Arg (Figures 3B and 3C). None of these mutations were present in the wild-type Columbia (Col), Landsberg *erecta*, or Wassilewskija accessions. In the course of our mapping, we sequenced all the
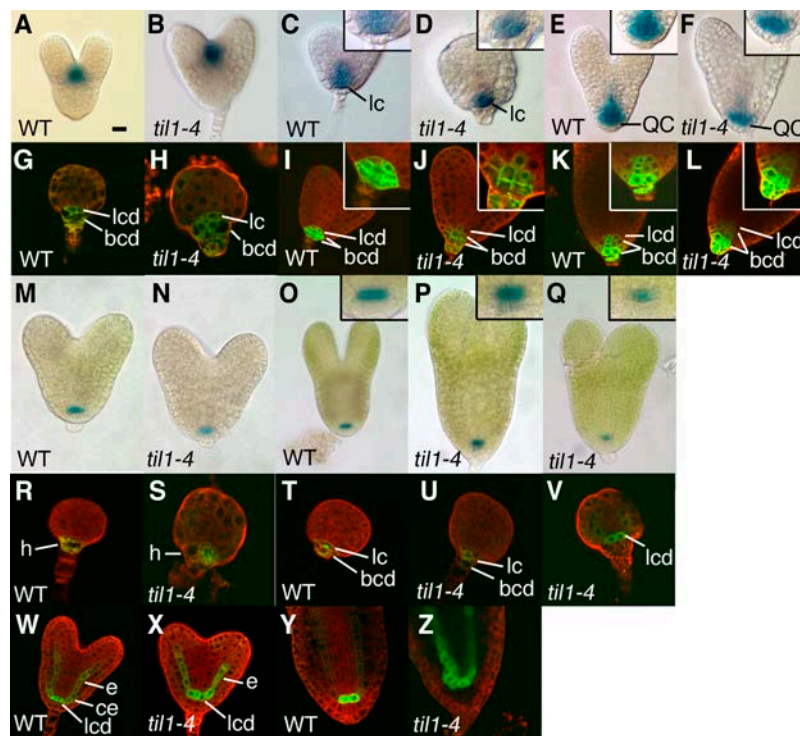
Figure 2. Expression of Cell-Specific Markers in Wild-Type and Homozygous *til1-4* Embryos.

The root pole is shown at higher magnification in the insets in **(C)** to **(F)**, **(I)** to **(L)**, and **(O)** to **(Q)**. h, hypophysis; lc, lens cell; lcd, lens cell descendants; bc, basal cell; bcd, basal cell descendants; ce, cortex-endodermis initials; e, endodermis. Bars = 10 μm in **(A)** to **(D)**, **(K)** to **(L)**, and **(W)** to **(Z)**, 15 μm in **(E)**, **(F)**, **(I)**, **(J)**, and **(O)** to **(Q)**, and 7.7 μm in **(G)**, **(H)**, **(M)**, **(N)**, and **(R)** to **(V)**.

(A) and **(B)** P_{STM}:*GUS* expression in wild-type **(A)** and *til1-4/til1-4* **(B)** heart stage embryos.

(C) to **(F)** *PIN4*:*GUS* expression in wild-type (**[C]** and **[E]**) and *til1-4/til1-4* (**[D]** and **[F]**) embryos. **(C)**, transition; **(D)**, late globular; **(E)** and **(F)**, late heart stages. In older mutant embryos **(F)**, *PIN4*:*GUS* expression is asymmetrically offset relative to the suspensor.

(G) to **(L)** *DR5rev*:*GFP* expression in wild-type (**[G]**, early globular; **[I]**, heart; **[K]**, torpedo stages) and *til1-4/til1-4* embryos (**[H]**, early globular; **[J]**, heart; **[L]**, torpedo stages). In the sections in **(J)** and **(L)**, a single lens cell descendant can be observed.

(M) to **(Q)** *QC25* expression in wild-type (**[M]**, early heart; **[O]**, torpedo stages) and *til1-4/til1-4* mutant embryos (**[N]**, early heart; **[P]** and **[Q]** torpedo stages). This expression highlights abnormalities in the lens cell lineage in mutants; the embryo in **(N)** has an abnormally shaped lens cell, while the embryo in **(Q)** has fewer lens cell descendants than the wild type.

(R) to **(Z)** P_{SCR}:*GFP* expression in wild-type (**[R]**, early globular stage; **[T]**, mid globular; **[W]**, heart; **[Y]**, torpedo stages) and *til1-4/til1-4* embryos (**[S]**, early globular; **[U]**, late globular; **[V]**, mid globular stages). Later in development, the normally U-shaped pattern of P_{SCR}:*GFP* expression is often asymmetric (**[X]**, heart; **[Z]**, torpedo stages), reflecting the lateral displacement of the root pole.

other open reading frames in the 44-kb interval and found no mutations in them. Altogether, the data indicated that TIL1 is encoded by *At1g08260*.

TIL1 is homologous to the large (catalytic) subunit of the eukaryotic DNA pol ε. *TIL1* encodes a gene that is annotated to be 15,949 bp, with 48 exons, accounting for an open reading frame of 6816 bp. It encodes a protein of 2271 amino acids, with a predicted molecular mass of 261 kD (www.arabidopsis.org). All the characteristic domains and subdomains of DNA pol ε (N-terminal, 3′–5′ exonuclease, 5′–3′ polymerase, proliferating cell nuclear antigen interaction, central, zinc-finger) are well conserved in TIL1 (Figure 3B; see Supplemental Figure 1 online). There is a second copy of the gene in the *Arabidopsis* genome, *TIL2* (*At2g27120*). TIL1 and TIL2 have been called At_DPOE1B/At POL2a and At_DPOE1A/At POL2b, respectively (Pospiech and Syväoja, 2003; Ronceret et al., 2005). The TIL2 protein

sequence is 79% identical (84% similar) to TIL1. The overall protein sequence identity/similarity of the homologue in rice (*Oryza sativa*) is 60%/71%. The identity/similarity of the protein compared with nonplant DNA pol εs ranges from 37%/55% (*S. cerevisiae* Pol2) to 41%/57% (*Homo sapiens* PolE1). The identity is higher in the N-terminal half of the protein (amino acids 1 to 1177), where most of the described domains reside, ranging from 50% (*S. cerevisiae* Pol2) to 87% (TIL2). The C-terminal domain is where the interactions with other subunits occur. These interactions may have diverged in different species, since *Schizosaccharomyces pombe* DNA pol ε catalytic subunit (*cdc20*) cannot rescue mutations in *S. cerevisiae Pol2* and vice versa (Sugino et al., 1998). The native DNA pol ε holoenzyme is a heterotetramer (Chilkova et al., 2003). Two of the three smaller subunits can be identified in *Arabidopsis* with a BLAST search. These are At5g22110 (subunit B, corresponding to DPB2 in
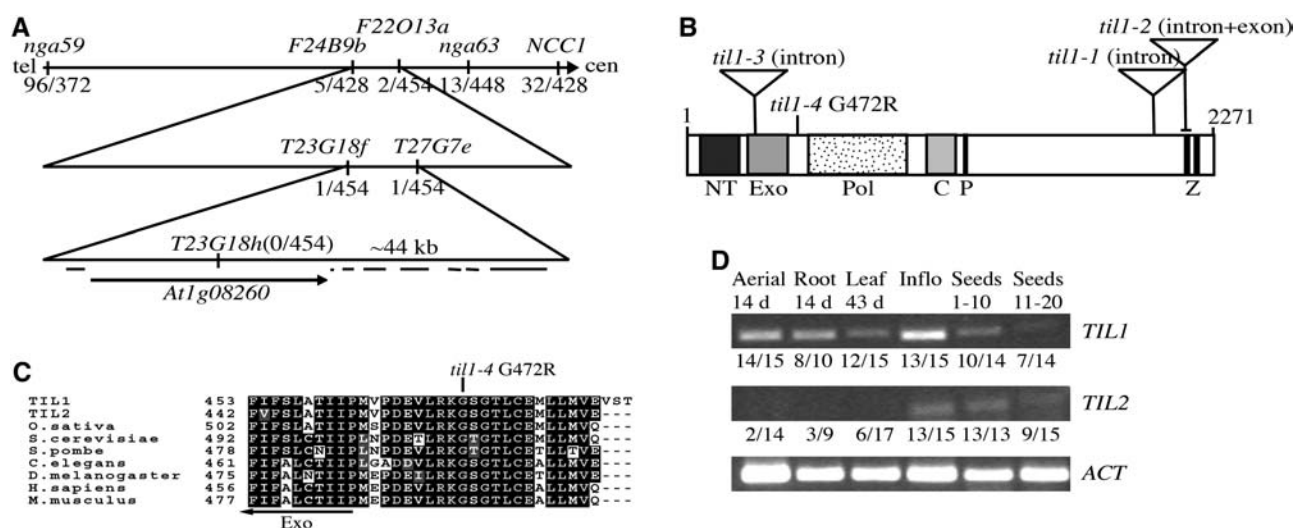
Figure 3. *TIL1* Encodes the Catalytic Subunit of DNA Pol ε.

(A) Map position of the *til1-4* mutation on chromosome I. The fractions shown indicate the number of recombinant chromosomes over the total number of chromosomes scored for each marker.
(B) Schematic of the TIL1 protein, showing the organization of its domains (NT, N-terminal; Exo, 3′-5′ exonuclease; Pol, 5′-3′ polymerase; C, central; P, proliferating cell nuclear antigen interaction; Z, zinc-finger). The position of the T-DNA insertions (*til1-1* to *til1-3*) and the point mutation (*til1-4*) are shown.
(C) Alignment of the region surrounding the amino acid residue altered by the *til1-4* mutation.
(D) Expression of *TIL1* and *TIL2* as determined by RT-PCR. The numbers under each lane indicate the fraction of times a band was detected. Actin was used as a control. Inflo, inflorescence; seeds 1-10, seeds from the first 10 siliques (to late heart stage); seeds 11-20, seeds from the next 10 siliques (torpedo stage to fully developed embryo).

S. cerevisiae) (Ronceret et al., 2005) and At1g09030 (subunit D, corresponding to DPB4 in *S. cerevisiae*). Subunit C may be represented by a small family of genes in *Arabidopsis*, the protein encoded by *At5g50490* being the closest one in sequence to DPB3 in *S. cerevisiae*.

All three T-DNA alleles (*til1-1* to *-3*) have the same embryonic lethal phenotype. Two of these alleles have insertions in introns: *til1-1* in intron 36 and *til1-3* in intron 7. The T-DNA in *til1-2*

Figure 4. Phenotypes of Embryos Carrying *til1* Insertion Alleles (*emb2284*) and of Double Mutants for *til1-1* and *til2-1*.

(A) *emb2284-1/emb2284-1* embryo arrested at early globular stage. Arrow shows abnormal division patterns. It also has an asymmetric lens cell.
(B) *emb2284-1/til1-4* heart stage embryo with a laterally displaced root pole.
(C) *emb2284-2/til1-4* early globular embryo with a longitudinally split hypophysis (arrow).
(D) Seed with a *til1-1/til1-1;til2-1/til2-1* embryo arrested as a zygote and a single endosperm nucleus (arrowhead).
lc, lens-shaped cell; rp, root pole; z, zygote. Bars = 10 μm in **(A)** to **(D)**.

straddles an intron–exon junction (47–48), and it has a deletion of amino acids 2150 to 2185 (see www.seedgenes.org for details) (Tzafrir et al., 2004). This deletion includes the first putative zinc-finger, which is involved in interactions with other subunits and is essential for viability in yeast (Dua et al., 1999) (Figure 3B; see Supplemental Figure 1 online). These data suggest that these alleles are functionally null. The mutation in *til1-4* produces a significant change in a residue that is conserved not only in all DNA pol ε catalytic subunits (Figure 3C) but also in the catalytic subunits of the other replicative DNA pols, δ and α (Huang et al., 1999). However, some enzymatic activity is likely retained, since *til1-4* homozygotes and *til1-4* trans-heterozygotes over the putative null alleles are viable.

We examined the expression of *TIL1* and *TIL2* in different tissues by RT-PCR. Both were expressed in most tissues at low levels. The levels were so low (particularly for *TIL2*) that we were not able to detect them in all the RT-PCR reactions for a particular tissue. The inflorescence (floral meristem and flowers until anthesis) was the tissue where the expression of both genes could be detected most consistently (Figure 3D). Interestingly, these DNA pols were expressed not only in actively dividing tissues but also in mature tissue (43-d-old leaves). An examination of the available microarray experiments confirms our results (www.genevestigator.ethz.ch) (Zimmerman et al., 2004). In globular stage embryos, *TIL1* is expressed at similar (low) levels in the apical and basal parts, while in heart stage embryos, it is expressed at a higher level in the rapidly growing cotyledons (Casson et al., 2005). In synchronized plant cells in culture, TIL1 shows its highest expression during the S-phase and a second
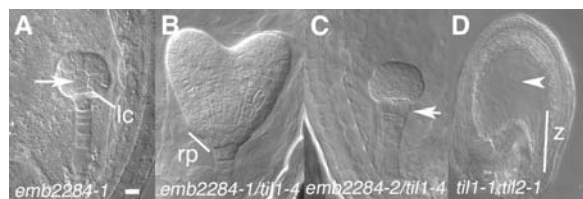
Table 5. Complementation Tests: Embryonic Phenotypes

	EMB2284/ emb2284-1 × TIL1/til1-4	TIL1/til1-4 × EMB2284/ emb2284-1	EMB2284/ emb2284-1 × TIL1/TIL1	TIL1/TIL1 × EMB2284/ emb2284-1	TIL1/TIL1 × TIL1/til1-4	TIL1/til1-4 × TIL1/TIL1	TIL1/TIL1 × TIL1/TIL1
Number of siliques	6	4	6	6	6	4	3
Number of embryos	243	144	247	186	211	144	79
Abnormal/delayed embryos	27%	23.6%	5.2%	4.3%	2.4%	4.9%	1.3%

lower peak at metaphase-anaphase. *TIL2* is expressed at constant low levels throughout the cell cycle (Menges et al., 2003; Ronceret et al., 2005).

til1 til2 Double Mutants Indicate That DNA Pol ε Is Essential for Cell Divisions in the Embryo and Endosperm

To determine whether *TIL1* and *TIL2* have redundant functions during embryo development, we obtained plant lines with T-DNA insertions in *TIL2*. The left border of the T-DNA in *til2-1* was at position 308 in intron 2 and caused a deletion of the last eight nucleotides of exon 2 and the first seven nucleotides of intron 2, while the left border of the T-DNA in *til2-2* was at position 9230 in exon 36 (see Supplemental Figure 1 online). Plants and embryos homozygous for either *til2* allele were wild-type in appearance. In the self progeny of *TIL1/til1-4;til2-1/til2-1* or *TIL1/til1-4;til2-2/til2-2* plants, we detected close to 25% of *til1-4/til1-4*–appearing embryos (16/74 and 26/90) and no new phenotypic classes. These results indicated that TIL2 is dispensable in the presence of wild-type TIL1 or TIL1-4. However, in the siliques of *TIL1/til1-1;til2-1/ til2-1* self-pollinated plants, we found that <1% of the embryos (3/367) had a *til1-1/til1-1*–like phenotype (globular arrest). Instead, almost 20% (68/367) of the embryos arrested much earlier in development, the majority of them at the zygote stage (57/367) (Figure 4D) or the one- to two-cell stage (6/367). In these seeds, the endosperm nucleus either did not divide (Figure 4D, arrowhead) or divided only once. Mutants for the unique *AtDPB2* subunit of the DNA pol ε complex (*cyclops2*) also show this phenotype (Ronceret et al., 2005). These data show that DNA pol ε is essential for all the cell divisions of the embryo and the endosperm. During the first six or seven rounds of embryonic cell division, *TIL1* and *TIL2* are at least partially redundant, as can be seen from the differences between the *til1-1/til1-1* and *til1-1/ til1-1;til2-1/til2-1* embryos (Figures 4A versus 4D).

Lengthening the Embryonic Cell Cycle with a DNA Pol Inhibitor Phenocopies *til1-4*

Embryos mutant for the *til1-4* allele showed a longer cell cycle and defects in root pole patterning. One hypothesis is that the change in cell cycle length is responsible for the morphological abnormalities. Another possibility is that both defects are independently caused by the *til1-4* mutation. We sought to distinguish between these alternatives by slowing down the embryonic cell cycles and then examining embryonic morphology. To do this, we treated wild-type embryos with aphidicolin, a well characterized drug that slows the S-phase of the cell cycle by competitively inhibiting all replicative DNA pols (α, δ, and ε) (Cheng and Kuchta, 1993; Wright et al., 1994). Aphidicolin induces a reversible S-phase block and is commonly used to synchronize plant cells in culture (Menges et al., 2003).

To treat the embryos, we staged and excised developing seeds from their siliques and cultured them on agar plates containing aphidicolin for 3 to 4 d (Sauer and Friml, 2004). After the treatment, we cleared the seeds and analyzed the embryonic morphology. Approximately 15% of untreated (control) embryos had root pole abnormalities that resembled those observed in *til1-4* homozygous embryos, while a smaller fraction had other defects (Figure 5A). These types of defects have been observed before in 10 to 20% of embryos cultured in the absence of drugs (Sauer and Friml, 2004). A dose of 5 μg/mL of aphidicolin had no effect on embryo development. Doses of 10 or 20 μg/mL had similar effects, significantly lengthening the embryonic cell cycle, with a total 152/236 (66%) of the embryos being approximately two rounds of cell division behind the control embryos from the same silique (data not shown). Among the delayed embryos, we observed two classes. Of the embryos in which the lens cell had not formed by the beginning of the treatment (two-cell to early globular stages), 58% had root pole defects that

Table 6. Complementation Tests: Postembryonic Phenotypes

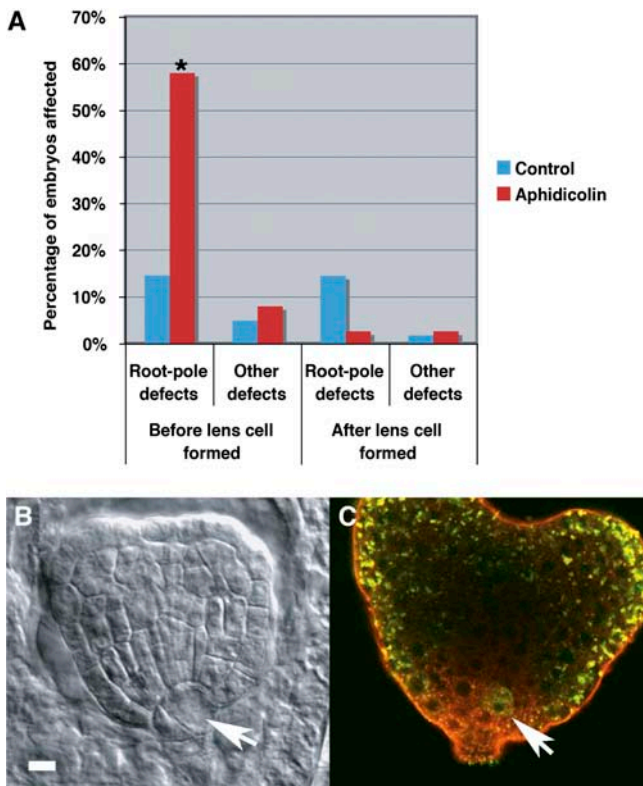|	Normal Fertility				
Phenotype Genotype (by PCR)	Normal Seeds *TIL1/TIL1*	Aborted Seeds *TIL1/emb2284-1*	Delayed Seeds *TIL1/til1-4*	Reduced Fertility *emb2284-1/til1-4*	Total
EMB2284/emb2284-1 × *TIL1/til1-4*	4 (23.5%)	4 (23.5%)	5 (29.5%)	4 (23.5%)	17
TIL1/til1-4 × *EMB2284/ emb2284-1*	7 (25%)	5 (18%)	9 (32%)	7 (25%)	28
Total	11 (24.4%)	9 (20%)	14 (31.1%)	11 (24.4%)	45

Figure 5. Treatment of Embryos with Aphidicolin.

(A) Graph of the percentage of embryos affected by treatment with aphidicolin. Embryos at two-cell to early globular embryo stages at the beginning of treatment were grouped in the "before lens cell formed" (control, $n = 144$; aphidicolin, $n = 113$), while embryos at later stages (to late globular stage) were grouped in the "after lens cell formed class" (control, $n = 55$; aphidicolin, $n = 39$). The observed morphological abnormalities were separated into root pole defects (til1-4-like) and other defects (other parts of the embryo). Asterisk indicates a significant difference with the control group (P < 0.01, Fisher's exact test).
(B) Transition stage embryo after aphidicolin treatement with an abnormally divided hypophysis (arrow).
(C) Early heart embryo after aphidicolin treatment showing an abnormally positioned P_{SCR}:GFP-expressing cell (arrow). The punctate green fluorescence is an artifact. Bar = 10 μm for **(B)** and **(C)**.

phenocopied til1-4 (Figures 5A and 5B). By contrast, <3% of the embryos in which the lens cell was present at the beginning of treatment (early to late globular stages) showed til1-4–like phenotypes (Figure 5A). Like til1-4/til1-4 embryos, a small fraction of aphidicolin-treated embryos presented defects in other regions of the embryo (Figure 5A). When we treated wild-type embryos transgenic for P_{SCR}:GFP with aphidicolin, the changes in its expression also mimicked what we observed in til1-4 (Figure 5C). We also measured treated embryos at the early heart stage and found that they were significantly larger than untreated embryos at that stage, also phenocopying til1-4 in this respect (Table 2).

Our results strongly suggest that the morphological abnormalities observed in til1-4 homozygous embryos are due to the lengthening of the S-phase of the cell cycle. They also indicate

a developmental window during which the hypophysis is susceptible to alterations in the cell cycle. After the division that generates the lens and basal cells had occurred, the patterning of the root pole was much less likely to be affected by the treatment.

The Average Cell Cycle in til1-4/til1-4 Embryos Is 35% Longer, and til1-4/til1-4 Embryos Pause at the Late Globular Stage

The data described above indicated that the cell cycle was longer in til1-4/til-4 embryos and that a mutant DNA pol was the cause for the slowdown. To be able to quantify more precisely the lengthening of the embryonic cell cycles, we manually pollinated TIL1/til1-4, TIL1/til1-1, or wild-type Col plants with self pollen and then collected two or three siliques per genotype at 8-h intervals. By clearing the developing seeds, we could stage all the embryos (see Supplemental Table 1 online). This allowed us to calculate the average number of cells per embryo at different time points for the different genotypes (the number of cells for each stage was from Jürgens and Mayer, 1994). We assigned the ~25% delayed embryos to the mutant category for the analysis. We plotted the number of cells versus time (hours after pollination [HAP]) using a $\log_2$ scale so that each unit increment represented a doubling of the number of cells (Figure 6). Phenotypically wild-type embryos (TIL1/TIL1 or TIL1/til1 in genotype) developed at the same constant pace in wild-type or heterozygous siliques, doubling their cell numbers approximately every 10 h (Figure 6). til1-4/til1-4 and til1-1/til1-1 embryos did not show an obvious delay with respect to the rest of the embryos in the silique until the two-cell stage (64 HAP) (see Supplemental Table 1 online). As the wild-type embryos progressed, the delay of the mutant embryos became much more evident. After the four-cell stage, til1-1/til1-1 embryos doubled their cell numbers at the same rate as the wild type, every 10.5 h. They arrested at the early to mid globular stage (as described above) and eventually aborted (Figure 6). By contrast, til1-4/til1-4 embryos developed at a slower pace, doubling their cell numbers every 13.4 to 13.7 h (Figure 6). Our data indicate that a missense mutation in DNA pol ε catalytic subunit (til1-4) causes a lengthening of the cell cycle, while the absence of gene function (til1-1) has no effect after the four-cell stage. One possible explanation for the difference between alleles is that in the complete absence of TIL1, TIL2 is able to compensate for part of the embryonic program (2- to 32-cell stages) (see above). TIL2 may not able to displace a defective TIL1-4 polymerase from the replication complex, hence slowing the rate of DNA synthesis.

In the same experiment, we followed the development of the endosperm. The triploid endosperm is the second product of the fertilization of the ovule and has the same genotype as the embryo. Both the til1-1/til1-1/til1-1 and til1-4/til1-4/til1-4 endosperms developed slower than the wild type, judging by a visible reduction in the number of syncitial nuclei when compared with wild-type endosperm at the same time point (Figures 1O and 1P). Some of those nuclei looked larger than their wild-type counterparts (Figures 1O and 1P, arrowheads). In both cases, the endosperm started to cellularize at about the same time as the wild-type endosperm, at ~120 to 128 HAP, when wild-type
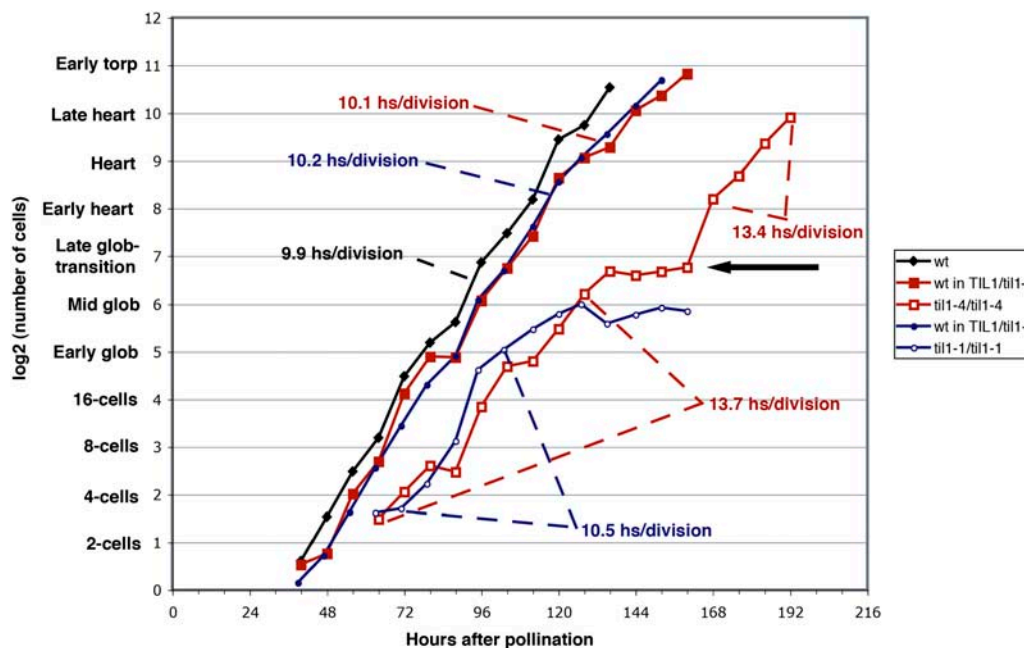
Figure 6. Cell Number in Wild-Type and *til* Mutant Embryos during Embryogenesis.

The three wild-type samples have similar cell doubling times. *til1-1/til1-1* embryos arrest at mid globular stage. *til1-4/til1-4* embryos develop slower than the wild type and pause at the late globular stage before continuing to develop (arrow). The data plotted are from Supplemental Table 1 online.

embryos were at the heart stage. The cell cycles (free nuclear cycles) in the mutant endosperm are therefore longer as well.

A surprising feature of the *til1-4/til1-4* embryos is that although they developed at a slower pace, the rate was not constant. The mutant embryos accumulated at around the late globular stage and paused for close to 24 h before moving on to the transition and heart stages (Figure 6, arrow). This pause was not seen in wild-type embryos and, to our knowledge, has not been described before. It would be interesting to explore whether this pause is a particularity of the *til1-4* allele or a more general phenomenon that is also present in other embryo-defective mutants.

DISCUSSION

Arabidopsis plants and embryos mutant for *til1-4*, a viable, missense mutation in DNA pol ε, show a lengthening of the cell cycle. The *til1-4* mutant embryos also exhibit cell fate changes that cause lateral displacement of the root pole from its normal position on top of the suspensor. This results in the shoot–root axis of the embryo being at an angle, or tilted, relative to the embryo-suspensor axis. Normally, these two axes are aligned in parallel. Our observations suggest that proper responses to early developmental signals at the embryonic root pole require a normal rate of progression through the cell cycle.

A Viable Mutation in DNA Pol ε Slows Down the Cell Cycle

Most of the mutational analyses of DNA pol ε have been done in yeast. Null alleles of DNA pol ε cause lethality in yeast as they do

in *Arabidopsis* (Figure 4; Kesti et al., 1999; Tzafrir et al., 2004; Ronceret et al., 2005). Viable mutant alleles of DNA pol ε cause yeast cells to have longer cell cycles, with an extended S-phase. This is presumably due to inefficient DNA synthesis or repair (Navas et al., 1995; Dua et al., 1999; Kesti et al., 1999; Feng and D'Urso, 2001). By analogy with the yeast mutants, the longer cell cycle we observe in *til1-4* mutants (Figure 6) may be due to a lengthening of the S-phase. Consistent with this, *TIL1* is expressed primarily during the S-phase (Menges et al., 2003; Ronceret et al., 2005), and the *til1-4* root pole defects can be phenocopied with the DNA pol inhibitor aphidicolin (Figure 5).

Few multicellular organisms that are mutant for replicative DNA pols have been described. *C. elegans* worms in which DNA pol δ or ε expression is inhibited by RNAi die as early embryos (Encalada et al., 2000; Fraser et al., 2000). Mice engineered to express an exonuclease-deficient version of DNA pol δ were viable and fertile, but they developed cancer after 2 months and died (Goldsby et al., 2001). Mutants with defective DNA pol α/primase also exist (Chen et al., 2000; Encalada et al., 2000; Gönczy et al., 2000). The scarcity of viable replicative DNA pol mutants points to the essential nature of these proteins and makes *til1* a rare and very useful mutant for the analysis of cell cycle–development interactions.

The Connections between Cell Cycle and Patterning during Embryogenesis

The reproducible set of cell divisions and patterning decisions during *Arabidopsis* embryogenesis suggests that the cell cycle, patterning, and morphogenesis are tightly coregulated. Severe

disruptions of the cell cycle or cell division result in very abnormal embryos (Hemerly et al., 2000; Yu et al., 2003). Mutations in genes involved in the origin of replication (*orc2*) or in chromosome integrity and separation (*ttn*) result in very early embryo and endosperm arrest. However, these arrest phenotypes are distinct from those of the absence of DNA pol ε. *orc2* embryos make several cells (Collinge et al., 2004), while *ttn* mutants embryos and endosperm have giant nuclei that we do not observe in *til1 til2* double mutants (Figure 4) (Liu and Meinke, 1998; Tzafrir et al., 2002, 2004).

Surprisingly, the effects on *Arabidopsis* embryonic patterning of lengthening the cell cycle by 35% in *til1-4* mutants are mostly limited to the hypophyseal lineage and the associated provasculature, and the embryos are viable. By contrast, a lengthening of the cell cycle by 25 to 50% in the *div-1* mutant in *C. elegans* results in absent cell types and lethality. In *C. elegans*, the correct timing and coordination of cell divisions is essential for the proper specification of cell fates (Encalada et al., 2000). Our data highlight the robustness and plasticity of plant development and suggest that the consequences of lengthening the cell cycle in *Arabidopsis* can be compensated for, to a certain degree, by the intercellular signaling mechanisms that regulate embryo patterning.

Why might the orientation and timing of the cell divisions of the hypophyseal lineage be so sensitive to a change in cell cycle length? The hypophysis is the only cell of the basal lineage that is incorporated into the developing embryo proper. It acquires a distinctive identity starting as early as the four-cell embryo proper stage (Haecker et al., 2004). Its first cell cycle is normally very long, since this cell does not divide (into the lens and basal cells) until the embryo proper is ∼32 cells (early globular stage). This division is asymmetric and requires a precise positioning of the spindle. The second cell cycle is also quite long. The lens and basal cells do not divide transversely until the embryo proper is ∼150 cells (transition stage) (Jürgens and Mayer, 1994). Coordination of the asynchronous cell cycles of the embryo proper and the hypophysis is likely required for the proper development of the hypophysis. In *til1-4*, the first division of the hypophysis occurs at the right developmental stage (early globular stage). However, the plane of division is abnormal in a majority of the embryos (being longitudinal in extreme cases), resulting in abnormally shaped and/or positioned derivatives. By contrast, the longitudinal division of the lens cell and the basal cell occurs too early (globular instead of transition stage), even in the cases where the plane of the first division is relatively normal (Figure 1, Table 1).

One hypothesis to explain these defects is that there are signals regulating the timing and/or orientation of the cell division of the hypophysis and derivatives that must be sent or perceived at a specific time in the cell cycle to be properly interpreted. There are several examples in other systems in which development is linked to the timing of cell cycle progression. The identities of the vulval cells in *C. elegans* and of prestalk/prespore cells in *Dictyostelium* are dependent on the phase of the cell cycle at which the precursors receive extracellular signals (Gomer and Firtel, 1987; Ambros, 1999). Also, gut-specific markers in the *C. elegans* embryo are not expressed unless the gut precursor cell (E cell) passes through the S-phase (Edgar and

McGhee, 1988). The same thing is observed for *even-skipped* expression in the ganglion mother cell GMC1-1a in *Drosophila* (Weigmann and Lehner, 1995). Preferentially lengthening the S-phase, as in the *til1-4* mutant or through aphidicolin treatment, may disrupt the relative positions in the cell cycle of the hypophysis and the cells sending the signals. This mismatch would then lead to the improper interpretation of these signals by the hypophysis. As a result, the cytoskeleton during the first cell cycle may be affected, resulting in misshapen cells or an improperly positioned division plane. The fact that the hypophysis remains sensitive to the aphidicolin treatment until approximately the time of division (Figure 5A) suggests that the putative signals are not received (or interpreted) until close to the end of this first cell cycle. The earlier than normal longitudinal division of the hypophysis derivatives in *til1-4* may be a consequence of the abnormal first division, or it may be the result of a later signal also being misinterpreted.

One of the main candidates for signaling between the embryo and the hypophysis is the hormone auxin. The current model for specification of lens cell (and later QC) identity in its proper position postulates the spatial intersection of two independent pathways, auxin and *SCR*, which integrate information about the apical–basal axis (auxin) and the radial axis (*SCR*) (Aida et al., 2004). *SCR* is not required for the division that generates a lens cell, just to determine its proper fate (Wysocka-Diller et al., 2000). In embryos mutant for the auxin response factor *monopteros* or its inhibitor *bodenlos*, the hypophysis does not develop properly (Berleth and Jürgens, 1993; Hamann et al., 1999). Neither gene is expressed in the hypophysis but in the cells directly above it (Hamann et al., 2002). Defects in the hypophysis, including abnormal planes of cell division and absence of a lens cell, are also seen in mutants that have impaired flow or response to auxin (*pin4*, *pin7*, P_{35S}:*PINOID*, *hobbit*, and *plethora*). Most of these mutants also fail to correctly specify the QC fate (Willemsen et al., 1998; Blilou et al., 2002; Friml et al., 2002, 2003, 2004; Aida et al., 2004). The abnormal cell divisions in the root pole of *til1* are reminiscent of those in mutants in the auxin pathway. However, auxin localization (as reported by *DR5rev*:*GFP*) is normal, and QC fate is specified (although off center) (Figure 2). Therefore, unlike mutants impaired in auxin response, the lengthening of the cell cycle in *til1* affects the orientation of the first cell division of the hypophysis but not the specification of the lcd as QC. Our data suggest that a signaling pathway distinct from auxin and *SCR* is involved in the defects observed in *til1* and that the orientation of the cell division plane that gives rise to the lens cell and its specification as QC are independently regulated processes.

til1 Affects the Placement of the Embryonic Root Pole

As discussed above, the primary defect in *til1* embryos is a lengthening of the cell cycle, which results in abnormal divisions of the hypophysis. How do these abnormal divisions translate into the abnormal positioning of the basal end of the shoot–root axis?

The hypophysis and its derivatives undergo a very reproducible set of cell divisions and, by the end of embryogenesis, give rise to the central part of the root pole: the QC and the columella.

Because of the orientation of the cell division planes, the QC is at the basal end of the embryo and directly on top of the suspensor and is surrounded by the initials (stem cells) of all the root tissue types: the columella, lateral root cap/epidermis, cortex/endodermis, and vasculature (Jürgens and Mayer, 1994; Scheres et al., 1994). There is evidence that during postembryonic root growth, signaling from the QC maintains the initials in an undifferentiated state (van den Berg et al., 1997; Sabatini et al., 2003) and that an ectopic QC can induce ectopic initials around it (Sabatini et al., 1999; Aida et al., 2004). Therefore, the QC acts as an organizer of the root meristem during postembryonic root growth. Recent results strongly suggest that the QC plays an organizer role during embryonic development (Aida et al., 2004). The key event in the setting up of the root pole is then the proper division of the hypophysis to make a lens cell (discussed above) and the specification of that cell and its derivatives as QC.

The phenotype of *til1* mutant embryos is variable in terms of degree of displacement of the QC with respect to the top of the suspensor. The primary defect appears to be an abnormal division of the hypophysis, which gives rise to abnormally positioned derivatives. The extent to which the root pole is affected may be related to the abnormality of the plane of first division of the hypophysis. At the globular stage, the position of the auxin maximum (as reported by *DR5rev:GFP*) is normal (Figure 2H). However, *SCR* expression is limited to one of the abnormal derivatives (Figure 2S). As postulated by Aida et al. (2004), the intersection of auxin and *SCR* appear to determine QC identity in that derivative. This fate is indicated by the expression of *PIN4* and *QC25* (Figures 2C to 2F and 2M to 2Q). This QC now is able to specify the tissue initials around it. Since the QC is off center due to that first abnormal division, the whole root meristem is shifted to one side by the heart stage (Figures 2F, 2J, and 2X). How abnormal the first division was determines the severity of the displacement of the root pole. The QC, once formed, is able to affect the distribution of auxin (Friml et al., 2002, 2003) so that the auxin maximum now is placed at the new root pole. Our results are consistent with the idea that the QC plays an organizing role for the root meristem during embryogenesis. This hypothesis also explains why other (more rare) abnormal divisions in *til1* embryos do not have long-term effects: those cells do not have organizing properties and instead respond to, and are corrected by, spatial signals from neighboring cells.

What remains to be explained is the asymmetric expression of *SCR* in the derivatives of the hypophysis, which ultimately determines the off-center position of the root pole. *SCR* acts autonomously in the lens cell, and its expression there is dependent on the movement of the SHORT ROOT (SHR) protein from the provasculature (Nakajima et al., 2001). One possibility is that, due to their asymmetric shape, the different derivatives of the hypophysis have different degrees of contact with the overlaying provascular cells. This may influence the amount of SHR protein that moves into them, which in turn may decide which cell expresses *SCR*. Heidstra et al. (2004) have proposed that in the future QC, once *SCR* expression is induced, it is autoregulated and becomes independent of *SHR*. This would help lock the QC fate in the chosen cell and, thus, the new position of the root meristem.

METHODS

Plant Material and Growth Conditions

The *til1-4* allele was isolated following ethyl methanesulfonate mutagenesis of a line containing a transgene with 3.3 kb of P_{STM}:GUS in a mixed Wassilewskija/Landsberg *erecta* background. Plants were screened for the segregation of aborted or delayed embryos (white seeds) (Joy, 2001). Plants segregating *til1-4* were outcrossed at least three times to wild-type plants (Col ecotype) before phenotypic analyses. The *til1-1*, *til1-2*, and *til1-3* T-DNA insertion alleles were isolated in a screen for embryo lethals (Col ecotype) and were previously named *emb2284-1* to *-3* (McElver et al., 2001; Tzafrir et al., 2004). The *til2-1* and *til2-2* alleles were obtained from the Salk collection of insertion alleles (SALK_092684 and SALK_056503) (Alonso et al., 2003). Unless specified, wild-type siblings were used as controls in all experiments. Transgenic cell-specific marker lines were generous gifts from J. Long (P_{SCR}:GFP), S. Woody (*PIN4*:GUS), B. Scheres (*QC25*), and J. Friml (*DR5rev*:GFP).

Plants were grown on commercial potting mix in greenhouses at 22 to 24°C under long-day conditions (16 h light/8 h darkness). When necessary, seeds were surface sterilized and germinated on agar plates (4.4 g/L Murashige and Skoog [MS] salts, 0.5 g/L MES, 10 g/L sucrose, 1× Gamborg's B5 vitamins, and 7.5 g/L agar, pH 5.7) supplemented with antibiotics (50 μg/mL kanamycin or 15 μg/mL gluphosinate ammonium) in incubators at 22°C, constant illumination. All chemicals were from Sigma-Aldrich or Fisher Scientific unless indicated.

For treatment with aphidicolin, developing seeds were cultured on agar plates as described by Sauer and Friml (2004). Plates were supplemented with aphidicolin (5 mg/mL stock in DMSO) or an equivalent volume of DMSO. Siliques were surface sterilized and slit open, and a few seeds were cleared in Hoyer's solution (see below) to determine the embryonic stage. The rest of the seeds were split between the treatment and control plates. The plates were covered in aluminum foil and incubated 3 to 4 d at 22°C. At the end of the experiment, seeds were either cleared in Hoyer's solution or the embryos were dissected out for confocal microscopy (see below).

Microscopy and Histochemistry

For morphological characterization, whole developing seeds were cleared in Hoyer's solution (70% chloral hydrate, 4% glycerol, and 5% gum arabic) and examined with differential interference contrast optics on a Nikon Eclipse E600 microscope. A similar protocol was used to clear dissected mature embryos and seedlings for cell counting. Photographs were taken with a Spot RT Slider camera (Diagnostic Instruments). Measurements of the embryo were done on ImageJ 1.33u (http://rsb.info.nih.gov/ij/). For confocal microscopy and histochemical staining, we dissected the embryos out of the ovules with tungsten microneedles (Fine Science Tools) in 10% glycerol and then transferred them to the appropriate solution. Staining for GUS was done at 37°C for several hours to overnight (depending on the marker) in 100 mM phosphate buffer, pH 7, 1 mM EDTA, 1% Tween-20, 2.5 mM potassium ferro/ferricyanide, and 1 mg/mL X-glucuronic acid (Rose Scientific). For the analysis of nuclear size and DNA content, embryos were mounted in 2 μg/mL DAPI in MS-glucose (4.4 g/L MS salts, 0.5 g/L MES, and 475 mM glucose, pH 5.7) and photographed using epifluorescence with the appropriate filter sets (excitation 330 to 380 nm; emission 435 to 485 nm). Nuclear size and fluorescence intensity measurements were taken using both ImageJ 1.33u and Phoretix 2D Evolution (Nonlinear USA) (with background subtraction set at "average on boundary"), with equivalent results. Nuclear volume was determined by measuring nuclear area and assuming that the nucleus was spherical. For confocal microscopy, embryos were mounted in MS-glucose with 33 μg/mL Nile Red as counterstain and imaged on a Bio-Rad MRC 1024/Nikon Diaphot 200 microscope (GFP, excitation 488 nm and emission 322/335 nm; Nile Red, excitation 568 nm

and emission 585 nm long pass). The brightness and contrast of all images were adjusted in Photoshop 7.0 (Adobe Systems).

Molecular Cloning and Expression Analysis

To map the *til1-4* mutation, a *TIL1/til1-4* M2 plant was crossed to a wild-type Col plant. Resulting F1 plants were allowed to self-fertilize, and the F2 progeny were scored for the segregation of *til1-4* and for segregation of PCR-based markers as described by Lukowitz et al. (2000) and in Results. The markers have been submitted to The Arabidopsis Information Resource (www.arabidopsis.org).

To determine the genotype of individual plants at the *TIL1* or *TIL2* locus, we used the PCR primers listed in Supplemental Table 2 online.

The expression of *TIL1* and *TIL2* in different tissues was analyzed by RT-PCR. For total RNA extraction from quick frozen tissue, the RNeasy plant mini kit (Qiagen) was used, followed by digestion with DNase I (DNA-free; Ambion). Two micrograms of RNA were used as template for reverse transcription (RETROscript; Ambion). PCR was performed using 5 μL of the 200-μL RT reaction, in a 50-μL reaction volume with SuperTaq (Ambion). The primers used (at 0.4 μM) were as follows: for *TIL1*, 5′-TCTTACCTAATGTAGCTTGC-3′ and 5′-AGGGCCATATATGATCC-AAG-3′; for *TIL2*, 5′-CTTGCAGCAACTGCGG-3′ and 5′-CCCTCTGTCTC-ACCATCTGG-3′; for actin, 5′-GAAGAACTATGAATTACCCGATGGGC-3′ and 5′-CCCGGGTTAGAAACATTTTCTGTGAACG-3′. We used 35 cycles (94°C for 45 s, 53°C for 45 s, and 72°C for 80 s). The DNA sequence of RT-PCR products was determined to confirm their identity.

Accession Numbers

Sequence data from this article can be found in the GenBank/EMBL data libraries under the following accession numbers: TIL1, NP_172303; TIL2, NP_180280; *C. elegans* (F33H2.5), NP_493616; *D. melanogaster* (dPOLE), NP_524462; *H. sapiens* (POLE1), AAP12650; *M. musculus* (POLE1), AAH63246; *S. cerevisiae* (Pol2), P21951; *S. pombe* (Cdc20), NP_596354; *O. sativa*, XP_465943.

Supplemental Data

The following materials are available in the online version of this article.

Supplemental Figure 1. Alignment of DNA Polymerase ε Protein Sequences.

Supplemental Table 1. Time Course of Wild-Type and Mutant Embryogenesis.

Supplemental Table 2. PCR Primers for Genotyping *til1* and *til2*.

REFERENCES

Aida, M., Beis, D., Heidstra, H., Willemsen, V., Blilou, I., Galinha, C., Nussaume, L., Noh, Y.-S., Amasino, R.M., and Scheres, B. (2004). The *PLETHORA* genes mediate patterning of the *Arabidopsis* root stem cell niche. Cell **119,** 109–120.

Alonso, J.M.A., et al. (2003). Genome-wide insertional mutagenesis of *Arabidopsis thaliana.* Science **301,** 653–657.

Ambros, V. (1999). Cell cycle-dependent sequencing of cell fate decisions in *Caenorhabditis elegans* vulva precursor cells. Development **126,** 1947–1956.

Barrôco, R.M., Van Poucke, K., Bergervoet, J.H.W., De Veylder, L., Groot, S.P.C., Inzé, D., and Engler, G. (2005). The role of the cell cycle machinery in resumption of postembryonic development. Plant Physiol. **137,** 127–140.

Berleth, T., and Jürgens, G. (1993). The role of the *monopteros* gene in organizing the basal body region of the *Arabidopsis* embryo. Development **118,** 575–587.

Blilou, I., Frugier, F., Folmer, S., Serralbo, O., Willemsen, V., Wolkenfelt, H., Eloy, N.B., Ferreira, P.C.G., Weisbeek, P., and Scheres, B. (2002). The *Arabidopsis HOBBIT* gene encodes a CDC27 homolog that links the plant cell cycle to progression of cell differentiation. Genes Dev. **16,** 2566–2575.

Casson, S., Spencer, M., Walker, K., and Lindsey, K. (2005). Laser capture microdissection for the analysis of gene expression during embryogenesis of *Arabidopsis.* Plant J. **42,** 111–123.

Chen, X., Li, Q., and Fischer, J.A. (2000). Genetic analysis of the *Drosophila DNAprim* gene: The function of the 60-kD primase subunit of DNA polymerase opposes the *fat facets* signaling pathway in the developing eye. Genetics **156,** 1787–1795.

Cheng, C.-H., and Kuchta, R.D. (1993). DNA polymerase ε: Aphidicolin inhibition and the relationship between polymerase and exonuclease activity. Biochemistry **32,** 8568–8574.

Chilkova, O., Jonsson, B.-H., and Johansson, E. (2003). The quaternary structure of DNA polymerase ε from *Saccharomyces cerevisiae.* J. Biol. Chem. **278,** 14082–14086.

Collinge, M.A., Spillane, C., Köhler, C., Gheyselinck, J., and Grossniklaus, U. (2004). Genetic interactions of an origin of replication complex subunit and the Polycomb group gene MEDEA during seed development. Plant Cell **16,** 1035–1046.

Davis, E.L., Rennie, P., and Steeves, T.A. (1979). Further analytical and experimental studies on the shoot apex of *Helianthus annuus*: Variable activity in the central zone. Can. J. Bot. **557,** 971–980.

Dua, R., Levy, D.L., and Campbell, J.L. (1999). Analysis of the essential functions of the C-terminal protein/protein interaction domain of *Saccharomyces cerevisiae* pol ε and its unexpected ability to support growth in the absence of the DNA polymerase domain. J. Biol. Chem. **274,** 22283–22288.

Edgar, L.G., and McGhee, J.D. (1988). DNA synthesis and the control of embryonic gene expression in *C. elegans.* Cell **53,** 589–599.

Encalada, S.E., Martin, P.R., Phillips, J.B., Lyczak, R., Hamill, D.R., Swan, K.A., and Bowermann, B. (2000). DNA replication defects delay cell division and disrupt cell polarity in early *Caenorhabditis elegans* embryos. Dev. Biol. **228,** 225–238.

Feng, W., and D'Urso, G. (2001). *Schizosaccharomyces pombe* cells lacking the amino-terminal catalytic domains of DNA polymerase epsilon are viable but require the DNA damage checkpoint control. Mol. Cell. Biol. **21,** 4495–4504.

Fraser, A.G., Kamath, R.S., Zipperlen, P., Martinez-Campos, M., Sohrmann, M., and Ahringer, J. (2000). Functional genomic analysis of *C. elegans* chromosome I by systematic RNA interference. Nature **408,** 325–330.

Friml, J., Benková, E., Blilou, I., Wisniewska, J., Hamann, T., Ljung, K., Woody, S., Sandberg, G., Scheres, B., Jürgens, G., and Palme, K. (2002). AtPIN4 mediates sink-driven auxin gradients and root patterning in *Arabidopsis.* Cell **108,** 661–673.

Friml, J., Vieten, A., Sauer, M., Weijers, D., Schwarz, H., Hamann, T., Offringa, R., and Jürgens, G. (2003). Efflux-dependent auxin gradients establish the apical-basal axis of *Arabidopsis.* Nature **426,** 147–153.

Friml, J., et al. (2004). A PINOID-dependent binary switch in apical-basal PIN polar targeting directs auxin efflux. Science **306,** 862–865.

Gendreau, E., Traas, J., Desnos, T., Grandjean, O., Caboche, M., and Höfte, H. (1997). Cellular basis of hypocotyl growth in *Arabidopsis thaliana*. Plant Physiol. **114,** 295–305.

Goldsby, R.E., Lawrence, N.A., Hays, L.E., Olmsted, D.A., Chen, X., Singh, M., and Preston, B.D. (2001). Defective DNA polymerase δ proofreading causes cancer susceptibility in mice. Nat. Med. **7,** 638–639.

Gomer, R.H., and Firtel, R.A. (1987). Cell-autonomous determination of cell-type choice in *Dictyostelium* development by cell-cycle phase. Science **237,** 758–762.

Gönczy, P., et al. (2000). Functional genomic analysis of cell division in *C. elegans* using RNAi of genes on chromosome III. Nature **408,** 331–336.

Haecker, A., Groß-Hardt, R., Geiges, B., Sarkar, A., Breuninger, H., Herrmann, M., and Laux, T. (2004). Expression dynamics of *WOX* genes mark cell fate decisions during early embryonic patterning in *Arabidopsis thaliana.* Development **131,** 657–668.

Hamann, T., Benkova, E., Bäurle, I., Kientz, M., and Jürgens, G. (2002). The *Arabidopsis BODENLOS* gene encodes an auxin response protein inhibiting MONOPTEROS-mediated embryo patterning. Genes Dev. **16,** 1610–1615.

Hamann, T., Mayer, U., and Jürgens, G. (1999). The auxin-insensitive *bodenlos* mutation affects primary root formation and apical-basal patterning in the *Arabidopsis* embryo. Development **126,** 1387–1395.

Heidstra, H., Welch, D., and Scheres, B. (2004). Mosaic analyses using marked activation and deletion clones dissect *Arabidopsis* SCARECROW action in asymmetric cell division. Genes Dev. **18,** 1964–1969.

Hemerly, A.S., Ferreira, P.C.G., Van Montagu, M., Engler, G., and Inzé, D. (2000). Cell division events are essential for embryo patterning and morphogenesis: Studies on dominant-negative *cdc2aAt* mutants of *Arabidopsis.* Plant J. **23,** 123–130.

Hobbie, L., McGovern, M., Hurwitz, L.R., Pierro, A., Liu, N.Y., Bandyopadhyay, A., and Estelle, M. (2000). The *axr6* mutants of *Arabidopsis thaliana* define a gene involved in auxin response and early development. Development **127,** 23–32.

Huang, D., Knuuti, R., Palosaari, H., Pospiech, H., and Syväoja, J.E. (1999). cDNA and structural organization of the gene *Pole1* for the mouse DNA polymerase ε catalytic subunit. Biochim. Biophys. Acta **1445,** 363–371.

Hübscher, U., Maga, G., and Spadari, S. (2002). Eukaryotic DNA polymerases. Annu. Rev. Biochem. **71,** 133–163.

Jakoby, M., and Schnittger, A. (2004). Cell cycle and differentiation. Curr. Opin. Plant Biol. **7,** 661–669.

Joy, R.E. (2001). *Arabidopsis* Embryonic Development: A Screen for Mutants Disrupted in Pattern Formation and Analysis of *BOBBER*, a Gene Required for Proper Specification of the Apical Region of the *Arabidopsis* Embryo. PhD dissertation (Madison, WI: University of Wisconsin).

Jürgens, G., and Mayer, U. (1994). Arabidopsis. In Embryos: Color Atlas of Development, J. Bard, ed (London: Wolfe Publishing), pp. 7–21.

Kesti, T., Flick, K., Keränen, S., Syväoja, J.E., and Wittenberg, K. (1999). DNA polymerase ε catalytic domains are dispensable for DNA replication, DNA repair, and cell viability. Mol. Cell **3,** 679–685.

Liu, C.-m., and Meinke, D. (1998). The titan mutants of Arabidopsis are disrupted in mitosis and cell cycle control during seed development. Plant J. **16,** 21–31.

Lukowitz, W., Gillmor, C.S., and Scheible, W.-R. (2000). Positional cloning in Arabidopsis. Why it feels good to have a genome initiative working for you. Plant Physiol. **123,** 795–805.

Mansfield, S.G., and Briarty, L.G. (1991). Early embryogenesis in *Arabidopsis thaliana.* II. The developing embryo. Can. J. Bot. **69,** 461–476.

Mayer, U., Büttner, G., and Jürgens, G. (1993). Apical-basal pattern formation in the *Arabidopsis* embryo: Studies on the role of the *gnom* gene. Development **117,** 149–162.

McElver, J., et al. (2001). Insertional mutagenesis of genes required for seed development in *Arabidopsis thaliana.* Genetics **159,** 1751–1763.

Menges, M., Hennig, L., Gruissem, W., and Murray, J.A.H. (2003). Genome-wide gene expression in an *Arabidopsis* cell suspension. Plant Mol. Biol. **53,** 423–442.

Nakajima, K., Sena, G., Nawy, T., and Benfey, P.N. (2001). Intercellular movement of the putative transcription factor SHR in root patterning. Nature **413,** 307–311.

Nakamura, A., Higuchi, K., Goda, H., Fujiwara, M.T., Sawa, S., Koshiba, T., Shimada, Y., and Yoshida, S. (2003). Brassinolide induces *IAA5, IAA19,* and *DR5*, a synthetic auxin response element in *Arabidopsis*, implying a cross talk point of brassinosteroid and auxin signaling. Plant Physiol. **133,** 1843–1853.

Natesh, S., and Rau, M.A. (1984). The embryo. In Embryology of Angiosperms, B.M. Johri, ed (Berlin, New York: Springer-Verlag), pp. 377–443.

Navas, T.A., Zhou, Z., and Elledge, S.J. (1995). DNA polymerase ε links the DNA replication machinery to the S phase checkpoint. Cell **80,** 29–39.

Pollock, E.G., and Jensen, W.A. (1964). Cell development during early embryogenesis in *Capsella* and *Gossypium.* Am. J. Bot. **51,** 915–921.

Pospiech, H., and Syväoja, J.E. (2003). DNA polymerase ε—More than a polymerase. ScientificWorldJournal **3,** 87–104.

Reddy, G.V., Heisler, M.G., Ehrhardt, D.W., and Meyerowitz, E.M. (2004). Real-time lineage analysis reveals oriented cell divisions associated with morphogenesis at the shoot apex of *Arabidopsis thaliana.* Development **131,** 4225–4237.

Ronceret, A., Guilleminot, J., Lincker, F., Gadea-Vacas, J., Delorme, V., Bechtold, N., Pelletier, G., Delseny, M., Chabouté, M.-E., and Devic, M. (2005). Genetic analysis of two Arabidopsis DNA polymerase epsilon subunits during early embryogenesis. Plant J. **44,** 223–236.

Sabatini, S., Beis, D., Wolkenfelt, H., Murfett, J., Guilfoyle, T., Malamy, J.E., Benfey, P.N., Leyser, O., Bechtold, N., Weisbeek, P., and Scheres, B. (1999). An auxin-dependent distal organizer of pattern and polarity in the *Arabidopsis* root. Cell **99,** 463–472.

Sabatini, S., Heidstra, H., Wildwater, M., and Scheres, B. (2003). SCARECROW is involved in positioning the stem cell niche in the *Arabidopsis* root meristem. Genes Dev. **17,** 354–358.

Sauer, M., and Friml, J. (2004). *In vitro* culture of *Arabidopsis* embryos within their ovules. Plant J. **40,** 835–843.

Scheres, B., Wolkenfelt, H., Willemsen, V., Terlouw, M., Lawson, E., Dean, C., and Weisbeek, P. (1994). Embryonic origin of the *Arabidopsis* primary root and root meristem initials. Development **120,** 2475–2487.

Schwartz, B.W., Yeung, E.C., and Meinke, D.W. (1994). Disruption of morphogenesis and transformation of the suspensor in abnormal *suspensor* mutants of *Arabidopsis.* Development **120,** 3235–3245.

Shevell, D.E., Leu, W.-M., Gillmor, C.S., Xia, G., Feldmann, K.A., and Chua, N.-H. (1994). *EMB30* is essential for normal cell division, cell

expansion, and cell adhesion in *Arabidopsis* and encodes a protein that has similarity to Sec7. Cell **77,** 1051–1062.

Sugimoto-Shirasu, K., and Roberts, K. (2003). "Big it up": Endoreduplication and cell size control in plants. Curr. Opin. Plant Biol. **6,** 544–553.

Sugino, A., Ohara, T., Sebastian, J., Nakashima, N., and Araki, H. (1998). DNA polymerase ε encoded by $cdc20^+$ is required for chromosomal DNA replication in the yeast *Schizosaccharomyces pombe.* Genes Cells **3,** 99–110.

Torres-Ruiz, R., and Jürgens, G. (1994). Mutations in the *FASS* gene uncouple pattern formation and morphogenesis in *Arabidopsis* development. Development **120,** 2967–2978.

Traas, J., Bellini, C., Nacry, P., Kronenberger, J., Bouchez, D., and Caboche, M. (1995). Normal differentiation patterns in plants lacking microtubular preprophase bands. Nature **375,** 676–677.

Tzafrir, I., Dickerman, A., Brazhnik, O., Nguyen, Q., McElver, J., Frye, C., Patton, D., and Meinke, D. (2003). The *Arabidopsis* SeedGenes project. Nucleic Acids Res. **31,** 90–93.

Tzafrir, I., McElver, J., Liu, C.-m., Yang, L.J., Wu, J.Q., Martínez, A., Patton, D., and Meinke, D. (2002). Diversity of TITAN functions in Arabidopsis seed development. Plant Physiol. **128,** 38–51.

Tzafrir, I., Pena-Muralla, R., Dickerman, A., Berg, M., Rogers, R., Hutchens, S., Sweeney, T.C., McElver, J., Aux, G., Patton, D., and Meinke, D. (2004). Identification of genes required for embryo development in *Arabidopsis.* Plant Physiol. **135,** 1206–1220.

van den Berg, C., Willemsen, V., Hendriks, G., Weisbeek, P., and Scheres, B. (1997). Short-range control of cell differentiation in the *Arabidopsis* root meristem. Nature **390,** 287–289.

Weigmann, K., and Lehner, C.F. (1995). Cell fate specification by *even-skipped* expression in the *Drosophila* nervous system is coupled to cell cycle progression. Development **121,** 3713–3721.

Willemsen, V., Wolkenfelt, H., de Vrieze, G., Weisbeek, P., and Scheres, B. (1998). The *HOBBIT* gene is required for formation of the root meristem in the *Arabidopsis* embryo. Development **125,** 521–531.

Wright, G.E., Hübscher, U., Khan, N.N., Focher, F., and Verri, A. (1994). Inhibitor analysis of calf thymus DNA polymerase α, δ and ε. FEBS Lett. **341,** 128–130.

Wysocka-Diller, J.W., Helariutta, Y., Fukaki, H., Malamy, J.E., and Benfey, P.N. (2000). Molecular analysis of *SCARECROW* function reveals a radial patterning mechanism common to root and shoot. Development **127,** 595–603.

Yu, Y., Steinmetz, A., Meyer, D., Brown, S., and Shen, W.-H. (2003). The tobacco A-type cyclin, *Nicta;CYCA3;2*, at the nexus of cell division and differentiation. Plant Cell **15,** 2763–2777.

Zimmerman, P., Hirsch-Hoffmann, M., Hennig, L., and Gruissem, W. (2004). GENEVESTIGATOR. Arabidopsis microarray database and toolbox. Plant Physiol. **136,** 2621–2632.